

Collapse of the critical state in superconducting niobium

Ruslan Prozorov,^{1,*} Daniel V. Shantsev,^{2,3} and Roman G. Mints⁴

¹Ames Laboratory and Department of Physics & Astronomy, Iowa State University, Ames, Iowa 50011

²Department of Physics, University of Oslo, P. O. Box 1048 Blindern, 0316 Oslo, Norway

³A. F. Ioffe Physico-Technical Institute, Polytekhnicheskaya 26, St. Petersburg 194021, Russia

⁴School of Physics and Astronomy, Raymond and Beverly Sackler Faculty of Exact Sciences, Tel Aviv University, Tel Aviv 69978, Israel
(Dated: 10 July 2006)

Giant abrupt changes in the magnetic flux distribution in niobium foils were studied by using magneto-optical visualization, thermal and magnetic measurements. Uniform flux jumps and sometimes almost total catastrophic collapse of the critical state are reported. Results are discussed in terms of thermomagnetic instability mechanism with different heat removal channels.

Large jumps in magnetization, temperature, ultrasonic attenuation and resistivity have been observed in many superconducting materials since early 60s [1, 2, 3, 4, 5, 6]. Although no definitive mechanism has been identified, it is believed that such changes are caused by sudden redistribution of Abrikosov vortices triggered and supported by thermomagnetic instabilities [1, 2, 3, 7, 8, 9, 10, 11, 12]. Direct observations of flux jumps with miniature Hall probes [13, 14, 15, 16] and real-time magneto-optical imaging [3, 17, 18, 19, 20, 21] have confirmed precipitous propagation of flux into the specimen. Although some evidence of large - scale jumps exists [5, 13], direct observations of avalanche - like behavior have mostly found dendritic and branched finger-like patterns (on a macroscopic scale of the whole sample) or small jumps (few tens of micrometers) forming teardrop-shaped flux fronts [3, 14, 15, 18, 19, 20, 21].

Theoretically, dendritic avalanches are expected for thin films with high critical current density [7, 11, 12]. The problem is that dendritic avalanches are too small to result in the observed jumps of magnetization, M . If δM is a variation of magnetization during a flux jump, then the dendritic avalanches contribute $\delta M \lesssim 0.1M$ [19]. However, the observed changes are often much larger [16, 22] (also see Fig. 1). They must be associated with a more dramatic catastrophic change of the critical state when a nonuniform (Bean's) distribution of vortices suddenly collapses. In this paper we present direct observations of the catastrophic collapse of the critical state in niobium foils and provide evidence for thermomagnetic origin of this effect.

Pure Nb (99.99%) strips of various thickness (5, 10 and 25 μm) were obtained from *Goodfellow*. Sample widths varied from 0.7 to 4 mm and the lengths varied from 2 to 10 mm. Magnetization loops, $M(H)$, were measured in a *Quantum Design* MPMS. Resistivity, specific heat and transport critical current were measured in a *Quantum Design* PPMS. We also measured sample temperature variation in quasi-adiabatic conditions and found temperature jumps associated with the flux jumps.

Figure 1 shows $M(H)$ in a 25 μm thick Nb foil at different temperatures, (a) 1.8 K, (b) 3 K and (c) 4 K. At

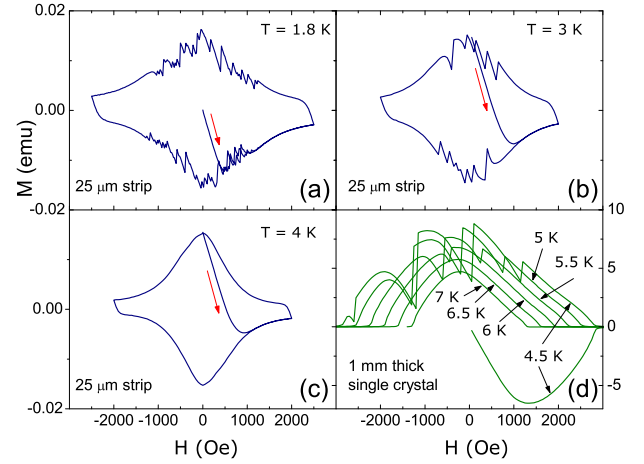


FIG. 1: (color online) Magnetization loops measured in 25 μm Nb foil at different temperatures, (a) 1.8 K, (b) 3 K, (c) 4 K and, for comparison, several $M(H)$ curves measured from 4 kOe to -4 kOe in large Nb single crystal. For (b) and (c) curves start from remanent magnetization, see text for details.

the lowest temperature, Fig. 1(a), jumps in $M(H)$ are observed both upon penetration after cooling in zero-field (ZFC) and upon flux exit. At larger temperatures, jumps were only observed upon reduction of the magnetic field, (b), and no jumps were observed above 4 K, (c). In Fig. 1(b) and (c) curves are shown after the external field was reduced from 5 kOe to zero and an attempt was made to observe jumps upon increase of the magnetic field of the same orientation. Unlike the case of the opposite field, no jumps in $M(H)$ were observed in this case. These observations support thermomagnetic instability mechanism [1, 2]. For comparison with foils, Fig. 1 (d) shows measurements in a large Nb single crystal (5 mm diameter, 1 mm thickness) at several temperatures. At $T = 1.8$ K both ascending and descending branches of the magnetization are shown. For other temperatures only descending branches are plotted. Giant magnetization jumps were ob-

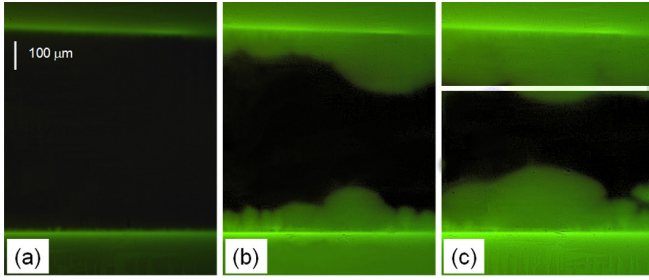


FIG. 2: (color online) Penetration of magnetic field in $10 \mu\text{m}$ thick Nb strip after zero-field cooling. (a) 160 (b) 360 (c) 480 Oe. Penetration in (b) and (c) was avalanche-like at fields indicated. (Real-time video at Ref. [25]).

served upon decrease of the magnetic field at temperatures up to 5.5 K. Evidently, variation of magnetization at a jump is much larger in the case of a large thick sample.

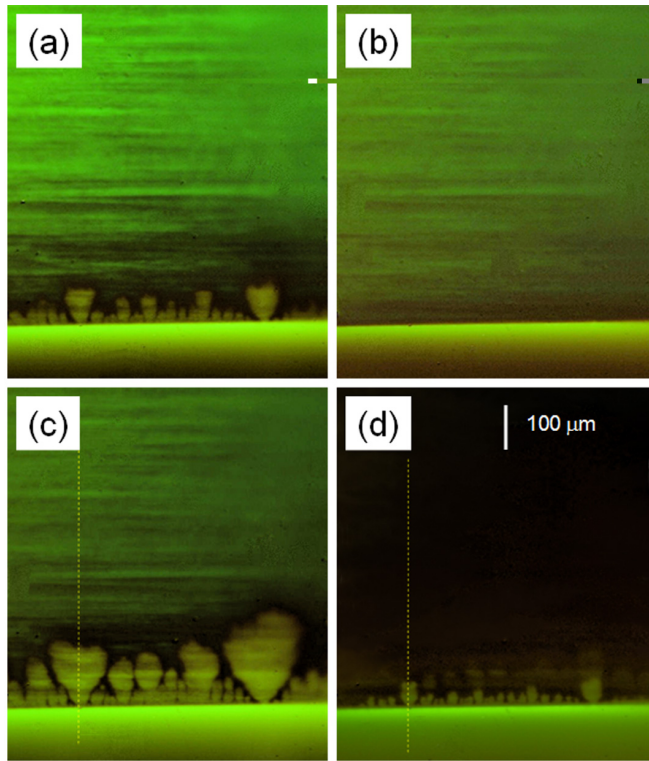


FIG. 3: Catastrophic collapse of the critical state upon entry of negative self-field at $T = 3.9 \text{ K}$. (a) 250 Oe (b) 200 Oe (c) 100 Oe (d) 50 Oe. (Real-time video at Ref. [25]).

Visualization of the magnetic induction, $B(r)$, on the sample surface was performed in a flow-type ^4He cryostat with the sample in vacuum attached to a copper heat exchanger. Bismuth-doped iron-garnet heterostructure film with in-plane magnetization was used as a magneto-optical indicator [23, 24]. In all images, intensity is proportional to the magnitude of $B(r)$. Moreover, due to the dispersion

of Faraday rotation for different wavelengths, up and down direction of magnetic fields can be distinguished. In our case, green corresponds to flux out of page and yellow corresponds to the opposite orientation (antiflux). This information is useful for flux-antiflux annihilation experiments, Fig. 5.

In magneto-optical experiments, sudden collapses of magnetization were observed only below $T \simeq 4.5 \text{ K}$ for all samples. Figure 2 shows penetration of the flux into a $10 \mu\text{m}$ Nb strip at increasing magnetic fields, (a) 160 Oe (b) 360 Oe and (c) 480 Oe. The large-scale abrupt jumps in Fig. 2 (b) and (c) occurred right before fields at which images were acquired (about 350 Oe and 470 Oe, respectively). In our case of 30 Hz data acquisition rate, the jumps seem instantaneous. Real-time dynamics can be viewed online [25].

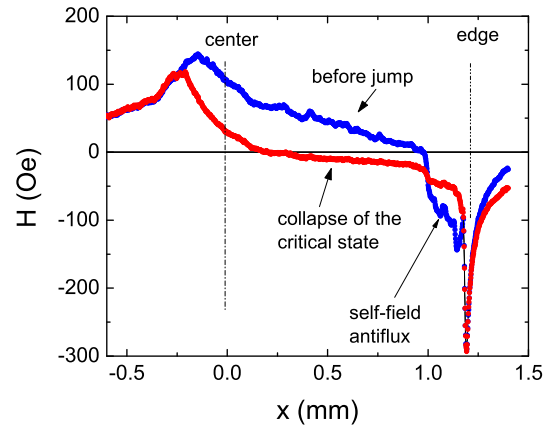


FIG. 4: (color online) Profiles of the magnetic flux before and after collapse of the critical state upon entry of the negative flux generated by self-field. The profiles were measured along dashed lines in Fig.3 (c) and (d).

The largest and most dramatic features occur upon decrease of a magnetic field when self-field antiflux starts to enter the sample (due to demagnetization factor). The antiflux annihilates with the trapped flux providing additional mechanism to trigger thermal instability. An avalanche in progress is difficult to stop, because the whole sample is in the critical state and an increase of temperature leads to reduction of the local critical current density resulting in further flux redistribution. This results in large uniform avalanches when the whole critical state literally collapses. In Fig. 3 two such collapses are shown, - panels (b) (jumped after (a)), and (d) (jumped after (c)). Some banding in Fig. 3 reflects the structure of the trapped flux in this sample. Note that flux collapse can reach over the center and cause apparent appearance of flux from the center if measured by a linear array of several Hall probes covering only part of the sample. This may explain reported

observations of dome-like features in Nb films [15].

Flux profiles corresponding to the collapse of the critical state are shown in Fig. 4. The profiles were measured along the dashed lines shown in Fig. 3 (c) and (d). Clearly, at some magnetic field, the slightest variation results in a change of the entire distribution of vortices. The observed giant jumps may span more than half the width of the sample, which, to the best of our knowledge, has never been observed before. Moreover, the collapse washes away both the interior critical state as well as any newly penetrated antflux at the edges. When the magnetic field of the opposite polarity is applied, antflux annihilates with the trapped flux similar to the self-field antflux discussed above. This results in large uniform avalanches as shown in Fig. 5. In general, the largest avalanches and sometimes total collapse of the critical state occurs at small fields upon entry of an antflux. We think that this is because critical current density is largest and most strongly field - dependent at low fields.

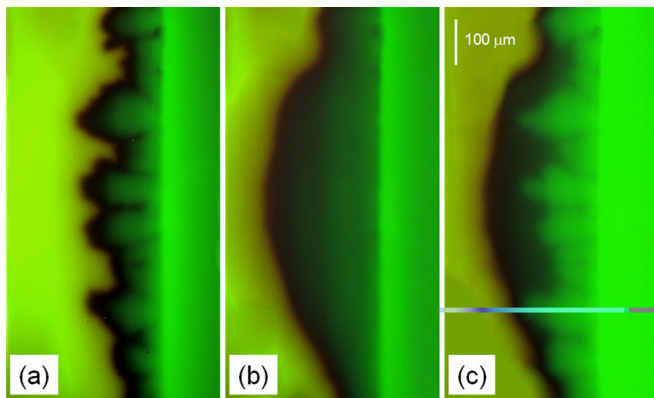


FIG. 5: Entry of the antflux (from right to left): (a) -320 Oe (b) -470 Oe. Note a huge uniform avalanche. (c) -740 Oe. Note secondary penetration on top of the flux distribution flattened by the avalanche. (Real-time video at Ref. [25]).

Although thermal instability seems to be the most natural scenario, direct evidence for thermal effects is scarce. Temperature jumps were detected in Nb-Zr alloys [4]. MgB_2 films coated with gold showed suppression of the dendritic avalanches [27]. We report direct measurements of the temperature variation associated with flux jumps in Nb foils. In this experiment, the sample was suspended by four wires on a thin sapphire stage normally used for specific heat measurements in a *Quantum Design* PPMS. The arrangement allows for direct reading of the sample thermometer in quasi-adiabatic conditions.

Figure 6 shows field sweeps (all taken from 3 kOe to -3 kOe). Temperature jumps were detected at the same range of temperatures and fields as magnetization measured in the same sample. To emphasize the variation, it was multiplied by a factor of 20. This provides clear evidence for thermal instability during uniform flux jumps.

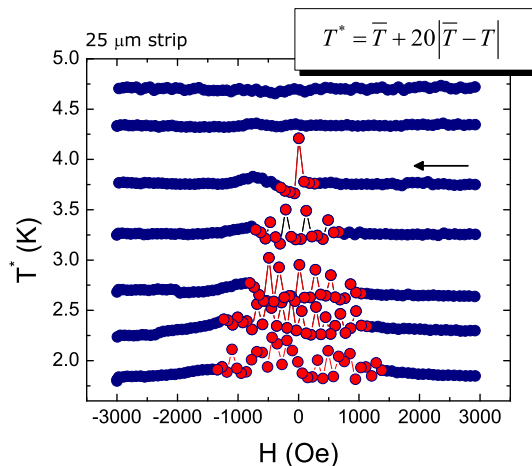


FIG. 6: (color online) Temperature variation upon decrease of magnetic field from 3 kOe to -3 kOe in a $25 \mu\text{m}$ thick Nb foil. The temperature variation was multiplied by a factor of 20 for clear visual appearance.

Assuming that all nonequilibrium magnetic energy $\delta Q = (\Delta B)^2 / 4\pi$ is absorbed by the material, the temperature variation $\delta T = \delta Q / C_p^v \simeq 0.03$ K, in agreement with direct measurements. Here, $C_p^v(T_0)$ is specific heat per unit volume and ΔB is the variation of the magnetic induction during the flux jump. In general, there are two channels to dissipate the energy of the critical state - dynamic and adiabatic [1, 2, 7]. The dynamic approach assumes that the heat redistribution is fast compared to the flux redistribution process. In this case the energy is removed to a coolant and the Joule heating is important if the dimensionless parameter, $\alpha = \rho j_c^2 d / h (T_c - T_0)$ is much larger than unity [7, 11]. Here j_c is the critical current, $h \simeq 1$ W/cm²K, is the heat transfer coefficient, $\rho \simeq 0.5 \mu\Omega\cdot\text{cm}$ is normal state resistivity, d - thickness and T_0 - temperature of the coolant. The adiabatic approach assumes that the field redistributes much faster compared to the heat redistribution process. In this case the energy is removed by the material itself by an increase of the temperature of the sample. The threshold parameter is given by $\beta = (\Delta B)^2 |dj_c/dT|_{T_0} / [4\pi C_p^v(T_0) j_c(T_0)]$, [1, 2]. With the numerical values obtained from direct measurements on our foils we obtain, $\alpha \simeq 30 - 50$ and $\beta \simeq 0.1 - 0.2$. These values indicate that dynamic channel is more significant, yet this value of α is marginal. Dendritic instability would require very large values ($\alpha \sim$ hundreds), so it seems that moderate values of α favor uniform flux jumps, in agreement with the experiment. A more detailed discussion of the instability threshold is given in Ref.[12].

The adiabatic approach can be used to estimate flux profiles after the uniform jump [10]. We assume that flux

jump stops when local current density becomes equal to the critical current density, j_c , which depends on the local temperature T . The flux jumps are assumed uniform along the flux front so that the problem becomes one-dimensional, but the non-locality of the $j(B)$ relation in thin films is taken into account. The input data for the model are measured $C_p(T) = 0.25 (T/T_c)^3$ J/mol-K and $j_c(T) = 1.5 \times 10^6 (1 - T/T_c)$ A/cm² and there were no free parameters. Measured (symbols, corresponding to Fig. 2) and calculated profiles (solid lines) of the magnetic induction are shown in Fig. 7. The magnetic induction profile at 300 Oe curve in Fig. 7 is calculated by using the standard Bean model for a thin strip [26]. For the 360 Oe curve we assumed that flux jumps occurred at 360 Oe and the initial profile was given by the Bean model. To obtain good fits, we had to use C_p values five times as large as the measured ones, which compensated for the large fraction of heat removed to the sample holder. This indicates the significance of the heat diffusion to a substrate, in agreement with above estimates for the priority of the dynamic channel. In addition, the experimental profile extends deeper into the sample than the calculated one indicating that lateral heat diffusion also takes place during the jumps. Apart from this, the model provides a good description of the induction profiles measured after flux jumps and therefore supports the thermal mechanism.

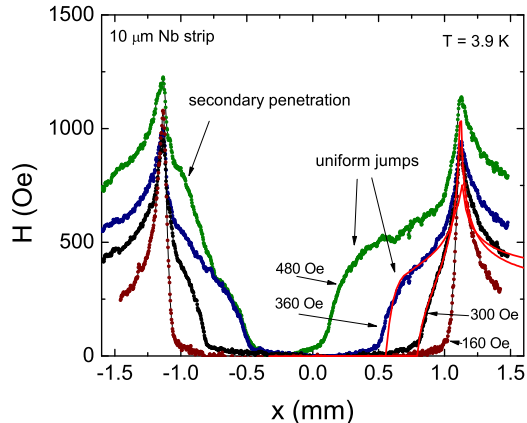


FIG. 7: (color online) Profiles of magnetic induction in 2.88 mm wide and 10 μm thick strip upon flux penetration after ZFC. Two inner profiles correspond to large uniform jumps shown in Fig. 2.

Furthermore, we tried to control the rate of heat conduction by introducing a thin mylar film between the heat exchanger and the sample. Both, teardrop-shaped protrusions and large uniform avalanches were observed in this case. Moreover, uniform jumps appeared even in ZFC samples where they were absent before. These experiments indicate that uniform avalanches occur at not too large heat link to

the thermal bath.

In conclusion, we observed large scale giant uniform vortex avalanches and even collapse of the critical state in niobium foils. Direct measurements of temperature variation as well as analysis of the magnetic and thermal energy balance support thermal instability scenario. Most likely, dynamic channel with moderate values of the stability parameter α leads to uniform flux jumps, but further work is needed to determine the area of parameters where dendritic flux avalanches change to uniform flux jumps.

We thank Alex Gurevich, Igor Aranson and Yuri Galperin for useful discussions and Thomas A. Girard for providing the samples and for discussions. Ames Laboratory is operated for US DOE by the Iowa State University under Contract No. W-7405-Eng-82. R. P. acknowledges support from NSF Grant DMR-05-53285 and from the Alfred P. Sloan Research Foundation.

* Electronic address: prozorov@ameslab.gov

- [1] R. G. Mints and A. L. Rakhmanov, *Rev. Mod. Phys.* **53**, 551 (1981).
- [2] A. V. Gurevich, R. G. Mints and A. I. Rahmanov, *"The Physics of Composite Superconductors"*, (Begell House Inc., New York, 1997).
- [3] E. Altshuler and T. H. Johansen, *Rev. Mod. Phys.* **76**, 471 (2004).
- [4] L. T. Claiborne and N. G. Einspruch, *J. App. Phys.* **37**, 925 (1966).
- [5] B. B. Goodman and M. Wertheimer, *Phys. Lett.* **18**, 236 (1965).
- [6] M. Levy *et al.*, *Phys. Rev. B* **2**, 2804 (1970).
- [7] I. S. Aranson *et al.*, *Phys. Rev. Lett.* **94**, 037002 (2005).
- [8] B. Biehler *et al.*, *Phys. Rev. B* **72**, 024532 (2005)
- [9] A. L. Rakhmanov *et al.*, *Phys. Rev. B* **70**, 224502 (2004).
- [10] D. V. Shantsev *et al.*, *Phys. Rev. B* **72**, 024541 (2005).
- [11] Y. E. Kuzovlev, cond-mat/0607143 (2006).
- [12] D. V. Denisov *et al.*, *Phys. Rev. B* **73**, 014512 (2006).
- [13] S. S. James *et al.*, *Physica C* **332**, 445 (2000).
- [14] E. Altshuler *et al.*, *Phys. Rev. B* **70**, 140505 (2004).
- [15] P. Esquinazi *et al.*, *Phys. Rev. B* **60**, 12454 (1999).
- [16] V. V. Chabanenko *et al.*, *Physica C* **369**, 82 (2002).
- [17] P. Leiderer *et al.*, *Phys. Rev. Lett.* **71**, 2646 (1993).
- [18] C. A. Durán *et al.*, *Phys. Rev. B* **52**, 75 (1995).
- [19] T. H. Johansen *et al.*, *Europhys. Lett.* **59**, 599 (2002).
- [20] M. S. Welling *et al.*, *Physica C* **411**, 11 (2004).
- [21] R. J. Wijngaarden *et al.*, *Euro. Phys. J. B* **50**, 117 (2006).
- [22] D. P. Young *et al.*, *Supercond. Sci. Technol.* **18**, 776 (2005).
- [23] A. A. Polyanskii, D. M. Feldmann and D. C. Larbalestier, in *"The Handbook on Superconducting Materials"*, D. Cardwell and D. Ginley, editors, UK, pp. 1551 (2003).
- [24] C. Jooss *et al.*, *Rep. Prog. Phys.* **65**, 651-788 (2002).
- [25] <http://cmp.ameslab.gov/supermaglab/video/Nb.html>
- [26] E. H. Brandt and M. Indenbom, *Phys. Rev. B* **48**, 12893 (1993).
- [27] Eun-Mi Choi *et al.*, *Appl. Phys. Lett.* **87**, 152501 (2005).